Lipotoxic heart disease in obese rats: Implications for human obesity

Yan-Ting Zhou*, Paul Grayburn*†, Asad Karim*†, Michio Shimabukuro*‡, Moritake Higa*, Dany Baetens§, Lelio Orci§, and Roger H. Unger*†¶

*Gifford Laboratories, Center for Diabetes Research, Department of Internal Medicine, University of Texas Southwestern Medical Center, 5323 Harry Hines Boulevard, Dallas, TX 75390; †Veterans Affairs North Texas Health Care System, 4500 South Lancaster Road, Dallas, TX 75216; ‡University of Ryukyus, 207 Uehara, Nishihara-cho, Okinawa 903-0125, Japan; and §Department of Morphology, University of Geneva Medical School, 1211 Geneva 4, Switzerland

Contributed by Roger H. Unger, December 9, 1999

To determine the mechanism of the cardiac dilatation and reduced contractility of obese Zucker Diabetic Fatty rats, myocardial triacylglycerol (TG) was assayed chemically and morphologically. TG was high because of underexpression of fatty acid oxidative enzymes and their transcription factor, peroxisome proliferator-activated receptor-α. Levels of ceramide, a mediator of apoptosis, were 2–3 times those of controls and inducible nitric oxide synthase levels were 4 times greater than normal. Myocardial DNA laddering, an index of apoptosis, reached 20 times the normal level. Troglitazone therapy lowered myocardial TG and ceramide and completely prevented DNA laddering and loss of cardiac function. In this paper, we conclude that cardiac dysfunction in obesity is caused by lipoapoptosis and is prevented by reducing cardiac lipids.

The recent increase in juvenile-onset obesity in the United States (1) predicts that the next generation of obese Americans will have been obese longer than ever before. This portends a higher prevalence of time-dependent complications of the disease, such as insulin resistance, non-insulin-dependent diabetes mellitus, hypertension, coronary artery disease, and other cardiac disorders. The etiology of these complications, which are often grouped together under the term "metabolic syndrome X" (2), is not known.

We have proposed that the excessive deposition of triacylglycerol (TG) in nonadipose tissues (steatosis) enlarges the intracellular pool of fatty acyl-CoA, thereby providing substrate for nonoxidative metabolic pathways, such as ceramide synthesis, that lead to cell dysfunction and death through apoptosis (3). It seemed possible that this sequence of events, established in the pancreatic islets of genetically obese Zucker Diabetic Fatty (ZDF) rats (*fa/fa*), could also take place in other tissues such as the heart.

Obesity-related heart disease, the most serious complication of human obesity, generally is attributed to coexisting disorders such as coronary artery disease and hypertension. Cardiac dysfunction, arrhythmias, cardiomyopathy, and congestive heart failure are seldom ascribed to the direct consequences of obesity, i.e., fatty acid (FA) overload of cardiac myocytes, although the literature does contain clinical reports of cardiomyopathy of obesity that can be reversed by weight loss (4).

This study was designed to test the possibility that the same metabolic abnormalities that cause lipotoxicity and lipoapoptosis in the pancreatic β cells of obese rats (3) might also compromise the function and viability of their myocardial cells. We used rats with obesity resulting from a loss-of-function mutation in the leptin receptor (5, 6), the ZDF (*fa/fa*) rat. We observed in their fat-laden hearts evidence of lipoapoptosis accompanied by a profound loss of cardiac function. These abnormalities were completely prevented by antisteatotic therapy. The striking benefit of such therapy on cardiac function in obese rats warrants an effort to determine whether a counterpart of this disorder exists in human obesity.

Materials and Methods

Animals. Male obese homozygous (*fa/fa*) ZDF rats and lean wild-type (+/+) littermates were bred in our laboratory from ZDF/Drt-*fa* (F_{10}) rats purchased from R. Peterson (University of Indiana School of Medicine, Indianapolis). All rats were fed standard laboratory chow (Teklad F6 8664; Teklad, Madison, WI) and given tap water ad libitum. Their genotype was determined as described by Phillips *et al.* (6).

At 7 weeks of age, homozygous obese prediabetic ZDF-Drt rats (*fa/fa*) were given powdered standard chow with or without a 6-week or a 13-week course of troglitazone (TGZ; 200 mg/kg per day; Sankyo). Body weight and food intake were measured weekly. Rats were sacrificed at 14 and at 20 weeks of age. Institutional guidelines for animal care and use were followed.

While the rats were under pentobarbital sodium anesthesia, nonfasting blood samples were obtained from the inferior vena cava. The heart was rapidly excised, and a portion of the left ventricle was frozen in liquid nitrogen and stored at −70°C for studies of mRNA and protein.

In some animals, the chambers of the heart were dissected and wet weights were determined.

Semiquantitation of mRNA by Reverse Transcriptase–PCR. Total RNA from heart tissue was extracted by the TRIzol isolation method (Life Technologies, Rockville, MD). RNA was treated with RNase-free DNase (Promega), and first-strand cDNA was generated from 1 μg of RNA in a 20-μl volume by using the oligo(dT) primer in the first-strand cDNA synthesis kit (CLONTECH). The PCR primers previously used for acyl-CoA oxidase (ACO) (7), liver carnitine palmitoyltransferase 1 (L-CPT-1) (8), the liver isoform of acetyl-CoA synthetase (8), glycerol-3-phosphate acetyltransferase (8), uncoupling proteins (8), peroxisome proliferator-activated receptor α (PPARα) (7), and β-actin cDNAs (8) again were used. The primers used for inducible nitric oxide synthase (iNOS) were 5′-CTGTGGTCACCTATCGCACC-3′ (forward), 5′-AGCCACATCCCGAGCCATGC-3′ (reverse), and 5′-TAGAGGTGGTCCTCCTCTGGGTGCCTGCAC-3′ (internal) (GenBank accession no. U03699). Levels of mRNA were expressed as the ratio of signal intensity for the target genes relative to that for β-actin. The PCR products were electrophoresed on an agarose gel and Southern blotting on a nylon membrane was carried out. Radiolabeled probes specific for each molecule were hybridized to the membrane and quantitated by a molecular imager (GS-363; Bio-Rad).

DNA Fragmentation Assay. DNA fragmentation was assayed by a modification of the method of Duke and Sellins (9), as described in detail (10).

Abbreviations: TG, triacylglycerol; TGZ, troglitazone; ZDF, Zucker Diabetic Fatty; FA, fatty acid; FFA, free fatty acid; ACO, acyl-CoA oxidase; L-CPT-1, liver carnitine palmitoyltransferase 1; GPAT, glycerol-phosphate acyltransferase; PPARα, peroxisome proliferator-activated receptor α; iNOS, inducible nitric oxide synthase.

¶To whom reprint requests should be addressed. E-mail: runger@mednet.swmed.edu.

The publication costs of this article were defrayed in part by page charge payment. This article must therefore be hereby marked "*advertisement*" in accordance with 18 U.S.C. §1734 solely to indicate this fact.

Table 1. Plasma lipid, glucose, and insulin levels in lean (+/+) and obese (*fa*/*fa*) ZDF rats

Rats	Age, wk	*n*	Substances measured			
			FFA, mM	TG, mM	Glucose, mM	Insulin, microunits/ml
Lean wild type (+/+)	7	3	0.33 ± 0.07	0.87 ± 0.12	4.97 ± 0.16	7.8 ± 1.5
	14	3	0.59 ± 0.31	0.99 ± 0.24	5.24 ± 0.22	7.6 ± 0.8
	20	3	0.61 ± 0.23	0.84 ± 0.08	5.54 ± 0.18	8.2 ± 1.2
Obese ZDF (*fa*/*fa*)	7	3	1.35 ± 0.37	1.1 ± 0.33	4.36 ± 0.2	35.6 ± 3.5
	14	6	2.02 ± 0.44*	6.27 ± 1.57*	12.22 ± 2.22*	121 ± 11.2*
	20	3	2.24 ± 0.58	8.98 ± 2.81	11.54 ± 2.77	59.5 ± 3
TGZ-treated (*fa*/*fa*)	14	6	1.28 ± 0.41†	1.59 ± 0.17†	5.11 ± 0.08†	31.7 ± 3.4†

*$P < 0.05$, untreated obese (*fa*/*fa*) rats vs. lean (+/+) rats.
†$P < 0.05$, 14-wk-old TGZ-treated obese (*fa*/*fa*) rats vs. untreated 14-wk-old obese (*fa*/*fa*) rats.

Ceramide Determination. Ceramide concentrations were measured in freshly isolated heart tissues from 7- and 14-week-old rats by a modification of the diacylglycerol kinase assay (11), as described in detail (10).

Analysis of Tissue Hydroxyproline and Protein Concentration. Left ventricular myocardial tissue from lean +/+ and obese *fa*/*fa* ZDF rats at 6 and 12 weeks of age (minimum $n = 5$ in each group) was weighed and a 5% homogenate was prepared. A sample (200 μl) of the homogenate was hydrolyzed under vacuum in 6 M HCl (110°C, 18 h). After reconstitution of the myocardial tissue in 2 ml of water, hydroxyproline concentration was determined by a colorometric assay. A portion of each homogenate was also used to measure myocardial protein concentration. Data were expressed as the ratio of total tissue hydroxyproline in μg/g of wet weight to the tissue protein in mg/g of wet weight.

Echocardiographic Evaluation of the Left Ventricle. At the age of 7, 14, and 20 weeks, obese prediabetic and diabetic rats (*fa*/*fa*) (minimum $n = 3$ at each time point), and lean control rats (+/+) at 20 weeks of age (minimum $n = 3$), were anesthetized with pentobarbital sodium and transthoracic echocardiographic examination was performed by using a Hewlett–Packard Sonos 5000 machine fitted with a 12-MHz transducer. M-mode and two-dimensional echo images were obtained in the parasternal long- and short-axis views. Doppler flow velocities across the mitral valve were obtained in the apical four-chamber view. The thickness of the interventricular septum and the posterior wall were determined in the parasternal long axis at the midchordal levels. Left ventricle dimensions (end-diastolic and end-systolic) were measured perpendicularly to the long axis of the ventricle at the midchordal levels. Fractional shortening was calculated as the end-diastolic dimension minus the end-systolic dimension divided by the end-diastolic dimension. Fractional area shortening was also calculated as the short-axis end-diastolic area minus the end-systolic area divided by the end-diastolic area. Transmitral Doppler velocities were measured at peak early filling and at atrial contraction. The mitral deceleration time was calculated as the time from peak early filling velocity to the time early filling returned to baseline. In the majority of rats, deceleration time could not be accurately calculated because of tachycardia.

TG Measurements in Heart Tissues. The hearts were dissected from rats, and then pieces were removed from the left ventricles. A solution (500 μl) of 2 mM NaCl/20 mM EDTA/50 mM sodium phosphate buffer, pH 7.4, was added to 0.5 g of left ventricle from which all pericardial adipose tissue had been meticulously removed by abrasion and scraping. Then, 10 μl of homogenate was mixed with 10 μl of *tert*-butyl alcohol and 5 μl of Triton X-100/methyl alcohol mixture (1:1 vol/vol) for the extraction of lipids. TGs were measured with a Sigma diagnostic kit.

Plasma Measurements. Rat blood samples were collected between 1:00 and 3:00 p.m. from the tail vein in capillary tubes coated with EDTA. Plasma glucose levels were measured by the glucose oxidase method with the Glucose Analyzer II (Beckman Coulter). Plasma insulin was assayed by standard methods with the Linco rat insulin kit (Linco Research Immunoassay, St. Charles, MO). Plasma free fatty acids (FFAs) were measured with the Roche FFA kit (Roche Diagnostics). Plasma TGs were measured by the method of Danno *et al.* (12).

Electron Microscopy and Quantification of Lipid Inclusions in Cardiac Muscle. Cardiac muscle fragments from the left ventricle were fixed with 2% glutaraldehyde in 0.1 M phosphate buffer (pH 7.4). After rinsing in phosphate buffer, postfixation in 1% osmic acid for 1 h at room temperature, and *en bloc* staining with uranyl acetate (13), specimens were processed for epoxy embedding (Polybed R812; Fluka). Thin sections were stained with uranyl acetate and lead citrate and photographed in a Philips CM 10 electron microscope (Philips, Eindhoven, The Netherlands). Morphometric analysis was performed on five different fragments of cardiac muscle (six fields per fragment) for each animal (three diabetic untreated and two TGZ-treated rats) and on three fragments (six fields per fragment) for each animal of three lean control rats. Volume density of lipid inclusions within the cardiac myocytes was determined by the point-counting method of Weibel (14). Data are mean ± SEM of 15 samples of cardiac tissue from untreated animals, 10 fragments from TGZ-treated animals, and 9 samples from lean controls.

Statistical Analysis. All data are presented as mean ± SEM. Statistical analyses were performed by using one-way or two-way analysis of variance (ANOVA), followed by Bonferroni's multiple comparison.

Results

Metabolic Features in Obese ZDF (*fa*/*fa*) Rats. The mean body weight, blood glucose, serum insulin, and plasma FFA and TG levels of obese male ZDF (*fa*/*fa*) rats were all greater than in age-matched lean male ZDF (+/+) controls at 7, 14, and 20 weeks of age (Table 1). FFA levels were 4 times the levels of lean controls, and they rose progressively to more than 2 mM, confirming earlier work (15). There was mild postprandial hyperglycemia at 7 weeks of age, which rose progressively to 380 ± 58 mg/dl at 20 weeks of age as the hyperinsulinemia declined from 121 ± 11.2 microunits/ml to 59.5 ± 3 microunits/ml. In the lean controls with normoglycemia, plasma insulin averaged 8.2 ± 1.2 microunits/ml.

Table 2. Cardiac weights and echocardiographic measurements in lean (+/+) and obese (*fa*/*fa*) ZDF rats at 20 weeks of age

Rats	*n*	Weights				Echocardiography				
		Body weight, g	Heart weight, g	RV weight, g	LV weight, g	LV end-diastolic diameter, mm	LV end-systolic diameter, mm	Septal wall thickness, mm	Posterior wall thickness, mm	Fractional shortening, %	Fractional area shortening, %
Lean wild type (+/+)	3	394 ± 6	1.20 ± 0.01	0.20 ± 0.01	0.85 ± 0.01	7.3 ± 0.3	4.2 ± 0.4	1.6 ± 0.1	1.9 ± 0.1	43 ± 6	65 ± 8
Obese ZDF (*fa*/*fa*)	8	572 ± 24*	1.55 ± 0.17	0.25 ± 0.02	1.06 ± 0.01	7.8 ± 0.7	5.0 ± 0.8*	1.6 ± 0.1	1.7 ± 0.2	36 ± 7*	56 ± 9*
TGZ-treated (*fa*/*fa*)	6	611 ± 7†	1.78 ± 0.29	0.24 ± 0.02	1.04 ± 0.02	7.6 ± 0.5	4.0 ± 0.6†	1.6 ± 0.1	1.8 ± 0.2	48 ± 7†	69 ± 7†

RV, right ventricle; LV, left ventricle.
*$P < 0.05$, untreated obese (*fa*/*fa*) vs. lean (+/+) rats.
†$P < 0.05$, TGZ-treated obese (*fa*/*fa*) vs. untreated obese (*fa*/*fa*) rats.

Fig. 1. Echocardiographic images from a normal lean ZDF (+/+) rat at age 20 weeks and an age-matched obese ZDF (*fa*/*fa*) rat. The dotted lines represent the cavity area for end-diastole (*Left*) and end-systole (*Right*). Both the end-diastolic and end-systolic areas are much larger in the *fa*/*fa* rat, indicating a dilated ventricle with subnormal systolic contraction.

Cardiac Features in Obese ZDF (*fa*/*fa*) Rats. The weight of the heart and its ventricles was greater in obese *fa*/*fa* rats than in lean +/+ controls at all ages studied, but only the left ventricular weight difference was statistically significant (Table 2). Echocardiography revealed a significant difference in end-systolic chamber size between the two groups at 20 weeks of age ($P < 0.04$; Table 2). Fractional area shortening, an index of contractile function, was significantly reduced in the 20-week-old obese *fa*/*fa* group ($P < 0.05$). A representative echocardiogram is displayed in Fig. 1.

Relationship of Cardiac Abnormalities to Myocardial TG Content. To determine whether the functional impairments observed in the hearts of the obese rats were related to the ectopic deposition of lipid in the myocardium, we compared the cardiac TG content of obese *fa*/*fa* rats with that of lean +/+ rats at 7 and 14 weeks of age. TG content was significantly higher than in controls at both age points (Fig. 2*a*). At 14 weeks, it was almost 3 times the controls' levels. Thus, substantial and progressively increasing cardiac steatosis was evident 6 weeks before the reduction in fractional area shortening was noted. This biochemical analysis of TG was confirmed morphometrically by determining the volume density of lipid droplets on electron micrographs of the myocardium of obese *fa*/*fa* rats (Fig. 2*b*). Such droplets were approximately 8 times as abundant as in lean +/+ control rats ($P < 0.001$).

Mechanism of the Myocardial Steatosis. In islets of obese *fa*/*fa* rats, the overaccumulation of TG is the result of increased esterification and impaired oxidation of the increased influx of FFAs (16, 17). We therefore semiquantified the mRNA of an enzyme of FA esterification, glycerol-phosphate acyltransferase (GPAT) (Fig. 3*A*), and two enzymes of FA oxidation, L-CPT-1 and ACO (Fig. 3 *B* and *C*). Cardiac GPAT mRNA, normalized for β-actin, was 35% higher than +/+ controls at 7 weeks of age and 160% higher at 14 weeks of age, consistent with increased lipogenesis. L-CPT-1 and ACO were reduced at both time points, suggesting reduced FA oxidation. Expression of PPARα, the transcription factor for ACO and L-CPT-1, was less than half that of +/+ controls (Fig. 3*D*), perhaps accounting for the underexpression of the enzymes of oxidation in the *fa*/*fa* group. There were no differences in liver acyl-CoA synthase (mRNA) (data not shown). Thus, the increased lipogenic capacity of the myocardium of *fa*/*fa* rats, like that of islets, may have resulted from overexpression of enzymes of FA esterification coupled with underexpression of enzymes of FA oxidation.

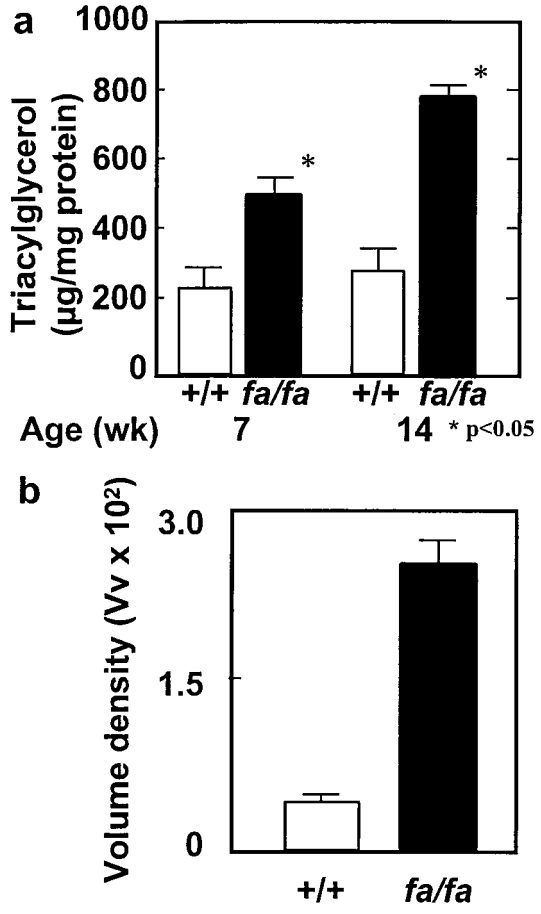

Fig. 2. (*a*) TG content in the myocardium of lean (+/+) and obese (*fa/fa*) ZDF rats at 7 and 14 weeks of age ($P < 0.05$). (*b*) Volume densities of lipid droplets in cardiac myocytes of lean (+/+) controls and obese (*fa/fa*) ZDF rats ($P < 0.001$).

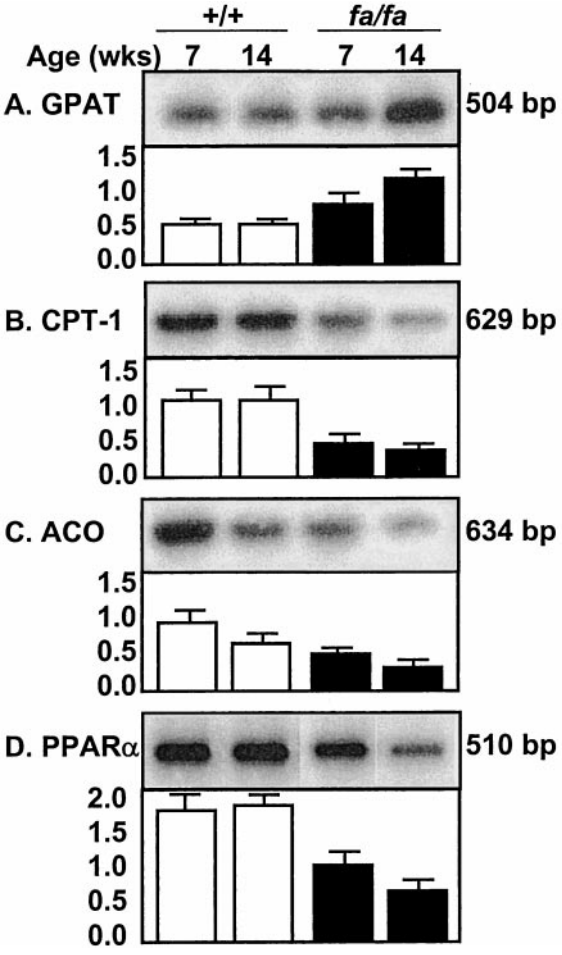

Fig. 3. Myocardial mRNA of L-CPT-1 (*B*) and ACO (*C*), enzymes of FA oxidation, and their transcription factor, PPARα (*D*), and an enzyme of FA esterification, GPAT (*A*). mRNA values were semiquantified by reverse transcriptase–PCR and normalized for β-actin mRNA.

Evidence of Myocardial Apoptosis. To determine whether cardiac steatosis, like steatosis in islets, culminates in apoptosis, we measured DNA laddering in the hearts of lean +/+ and obese *fa/fa* rats. Whereas DNA laddering in the +/+ control rats was only 0.8 ± 0.2% and 0.9 ± 0.2% at 7 and 14 weeks of age, respectively, in *fa/fa* rats it was greater than 5% at 7 weeks and approached 15% at 14 weeks (Fig. 4*a*). Moreover, the ratio of hydroxyproline to protein rose substantially during this period, from 0.57 ± 0.11 at 7 weeks of age to 0.82 ± 0.22 at 14 weeks of age ($n = 10$; $P < 0.01$), which is consistent with increasing fibrosis (data not shown). In +/+ controls, by contrast, the ratio of hydroxyproline to protein was 0.55 ± 0.13 at 7 weeks of age and 0.53 ± 0.09 at 14 weeks of age. Thus, cardiac steatosis, like hepatic and insular steatosis, is followed by a progressive increase in deposition of fibrous tissue.

Mechanism of Myocardial Apoptosis. In islets of obese *fa/fa* rats, the lipoapoptotic pathway involves an increase in *de novo* ceramide synthesis because of the overabundance of precursor long-chain FAs (18). To determine whether a similar mechanism occurs in the heart, we compared the myocardial ceramide content in the lean +/+ and obese *fa/fa* rats. In the latter group, there was a small but statistically significant increase at 7 weeks of age, whereas at 14 weeks of age, ceramide levels were twice those of the controls (Fig. 4*b*). By contrast, ceramide levels in the lean +/+ controls did not increase with age.

Ceramide-mediated apoptosis in islets involves up-regulation of the expression of iNOS (19), thereby augmenting the production of NO. We therefore semiquantified iNOS mRNA in obese *fa/fa* and lean +/+ rats. At 7 weeks of age, iNOS mRNA was twice the normal level and at 14 weeks of age, more than 4 times the normal level (Fig. 4*c*).

Effects of the Antisteatotic Agent TGZ. TGZ dramatically reduces the islet TG of obese *fa/fa* rats and prevents the β cell dysfunction and morphologic changes that otherwise occur (20). To obtain further support for a causal relationship between the myocardial steatosis and cardiac dysfunction, we treated obese *fa/fa* rats with the antisteatotic agent TGZ for 6 or 13 weeks, beginning at 7 weeks of age. Plasma FFA in treated rats was 34% below the untreated controls and plasma TG was 80% less than controls (Table 1). Myocardial TG content was 41% below untreated *fa/fa* controls (Fig. 5*a*). Morphometric quantification of lipid droplets (see Fig. 6) also revealed a large decrease (Fig. 5*b*). The elevation in ceramide content was prevented completely, and levels were similar to the +/+ lean controls (Fig. 5*c*). DNA laddering also was prevented completely and was less than that of 7-week-old *fa/fa* rats (Fig. 5*d*). There was no reduction in fractional area shortening (Fig. 5*e*), evidence that normal contractile function had been preserved by the therapy.

Discussion

Nonadipocytes have a very limited capacity to store excess fat (3). If they are exposed to high levels of plasma lipids, as usually

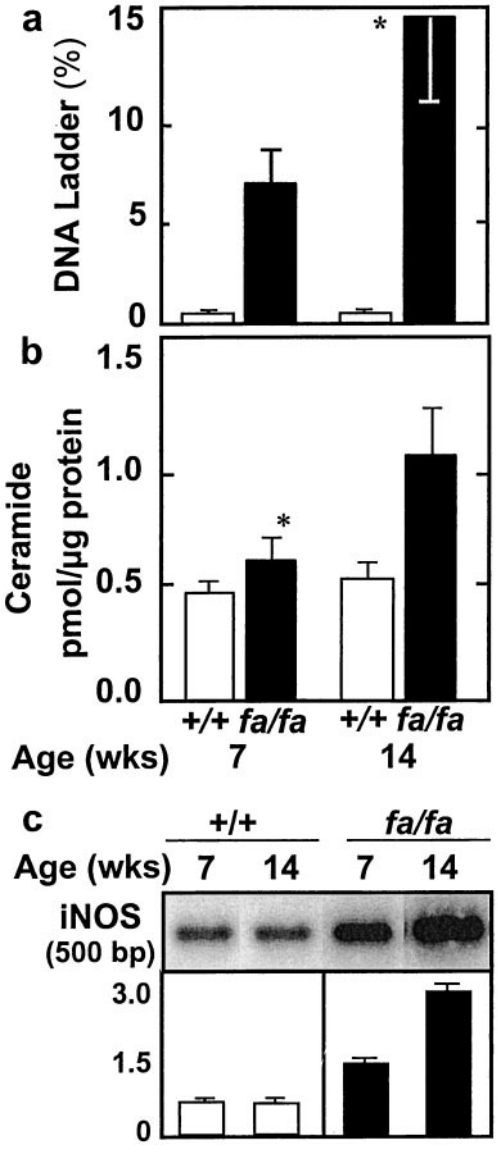

Fig. 4. (*a*) Percentage of myocardial DNA laddering, an index of apoptosis, obtained at 7 and 14 weeks of age in lean (+/+) and obese (*fa/fa*) ZDF rats (*, $P < 0.01$). (*b*) Myocardial ceramide levels in lean (+/+) and obese (*fa/fa*) ZDF rats at 7 and 14 weeks of age (*, $P < 0.01$). (*c*) Myocardial iNOS mRNA in lean (+/+) and obese (*fa/fa*) ZDF rats at 7 and 14 weeks of age.

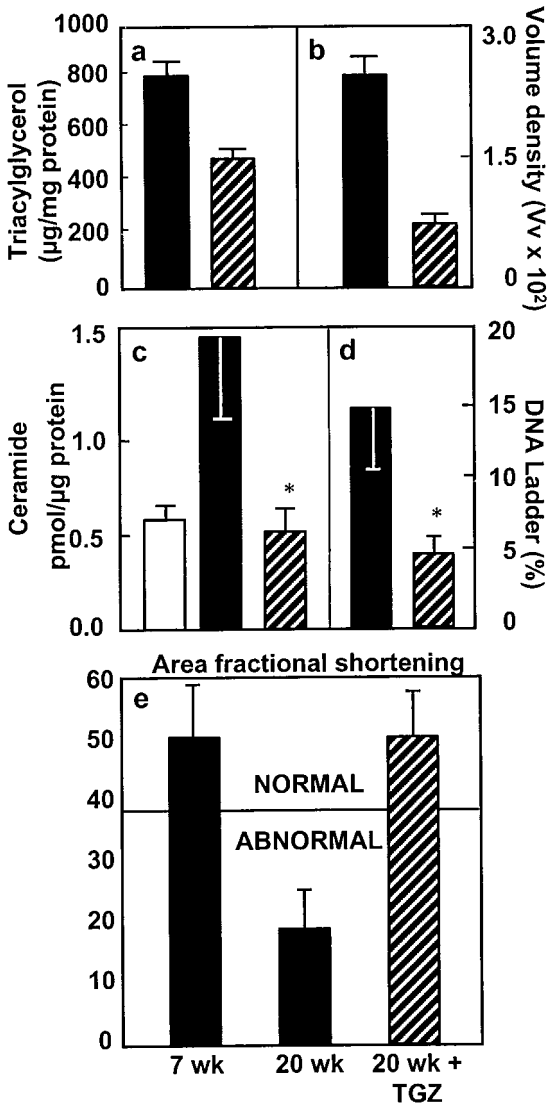

Fig. 5. (*a*) The effect of TGZ treatment on myocardial TG in obese (*fa/fa*) ZDF rats and untreated littermates ($P < 0.01$). (*b*) Morphometric quantification of lipid droplets in the myocardium of TGZ-treated obese ZDF rats and of untreated controls ($P < 0.001$). (*c*) Myocardial ceramide content in TGZ-treated and in untreated obese ZDF rats ($P < 0.01$). (*d*) Myocardial DNA laddering in TGZ-treated and untreated obese ZDF rats ($P < 0.01$). (*e*). Fractional area shortening, an index of myocardial contractile function, in TGZ-treated and untreated obese ZDF rats (*, $P < 0.01$; $n = 4$). □ = lean (+/+) rats; ■ = untreated ZDF (*fa/fa*) rats; ▨ = TGZ-treated ZDF (*fa/fa*) rats.

occurs in obesity, they may undergo steatosis and loss of function, and ultimately FA-induced "lipoapoptosis" may occur (3). In ZDF *fa/fa* rats, a model of obesity secondary to genetic unresponsiveness to leptin, TG accumulates rapidly in the heart, as it does in other nonadipose tissues, as the animals become increasingly obese. This is the consequence not only of elevated plasma lipids, but also of increased expression in nonadipose tissues of lipogenic enzymes such as GPAT, an enzyme of FA esterification, coupled with decreased expression of ACO and CPT-1, enzymes of FA oxidation, and their transcription factor, PPARα. These changes are associated with a progressive increase in ceramide content and iNOS expression. By 14 weeks of age, DNA laddering is increased markedly, evidence of severe cardiac apoptosis. At this time, left ventricular end-diastolic diameter has increased significantly. An associated increase in fibrous tissue in the myocardium is suggested by a rise in the hydroxyproline-to-protein ratio. Significant reduction in fractional area shortening is observed at 20 weeks of age, evidence of a clinically significant reduction in cardiac contraction.

Evidence here strongly suggests a causal link between the steatosis and the cardiac dysfunction. TGs themselves are probably inert, but their hydrolysis to fatty acyl-CoA provides increased substrate for ceramide synthesis. Ceramide up-regulates iNOS expression and increases NO production; the resulting increase in peroxynitrite is believed to cause the apoptosis (21). Just as the lipoapoptosis in pancreatic β cells of *fa/fa* rats was found to be secondary to an increase in *de novo* ceramide formation from the overabundance of unoxidized FAs (18), so the increase in myocardial ceramide content is likely to reflect *de novo* synthesis. The extent of the myocardial apoptosis and the accompanying secondary fibrosis observed in this study certainly could account for a loss of cardiac function. A causal relationship

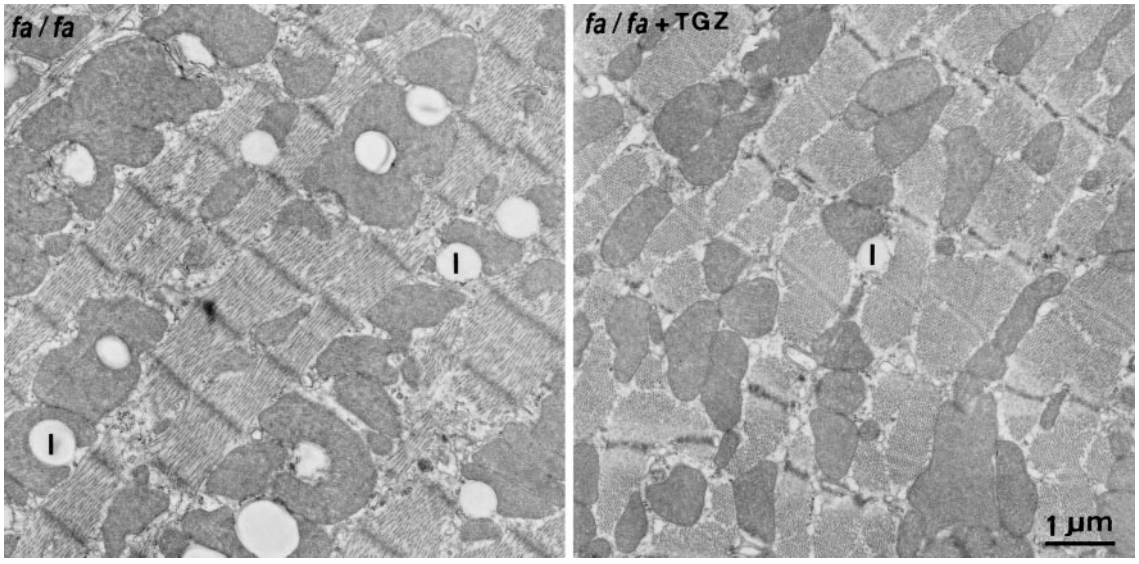

Fig. 6. Pair of thin sections of the myocardium of an 18-week-old untreated obese (*fa/fa*) ZDF rat (*Left*) and a TGZ-treated obese (*fa/fa* + TGZ) ZDF rat (*Right*). Note the reduction of lipid droplets (|) in TGZ-treated animals. The quantitative evaluation of the lipid accumulation is shown in Fig. 5*b*.

between the abnormal FA metabolism and the reduced myocardial contractility is further supported by the fact that TGZ, which reduced cardiac TG, prevented both the cardiac apoptosis and the loss of myocardial function.

The fact that myocardial iNOS mRNA was more than twice normal at 7 weeks of age and more than 4 times normal at 14 weeks of age raises the possibility that iNOS inhibitors might also be useful therapeutically in preventing the consequences of cardiac steatosis. We have reported that two iNOS inhibitors, aminoguanidine and nicotinamide, both completely prevented the consequences of islet steatosis (19). Thus, if a human counterpart of this cardiac lipotoxicity is identified, there are available agents that should be effective alone or in combination.

Whereas in ZDF rats both the obesity and ectopic overaccumulation of TG in nonadipose tissue are the result of a loss-of-function mutation in the leptin receptor (5, 6), in humans, the obesity is diet-induced rather than congenital. The initial years of human obesity are therefore usually free of complications, such as diabetes and heart disease, suggesting that protection by the leptin antisteatotic system is effective early on. Complications may appear later in the disease, but it remains to be determined whether they are the result of the same lipotoxic changes observed here in congenitally leptin-receptor-defective rodents. If so, it would indicate that a late failure of the antisteatotic system occurs in diet-induced obesity. Such failure could result from relative hypoleptinemia, from "system overload," in which the flux of FAs into the nonadipose tissues exceeds the capacity of the fully up-regulated oxidative machinery to handle, and/or from postreceptor leptin resistance.

At present, most clinicians attribute the cardiac derangements that occur in obesity to coronary artery disease or hypertension, because these are established diagnostic categories commonly associated with obesity. Nevertheless, it is possible that lipotoxic heart disease exists, both alone and in concert, with these well-recognized causes of heart disease and impairs the ability of the myocardium to compensate for them. If so, antisteatotic therapy might provide a valuable therapeutic adjunct in this increasingly common human disorder.

We thank Susan Kennedy and Kay McCorkle for secretarial support and Daniel Foster, M.D., and Ron Victor, M.D., for their critical review of this paper. We acknowledge the grant support of the Department of Veterans Affairs Institutional Support (SMI 821–109), the National Institutes of Health (DK02700–37), the National Institutes of Health/Juvenile Diabetes Foundation Diabetes Interdisciplinary Research Program, the Novo-Nordisk Corporation, and the Swiss National Science Foundation (L.O.).

1. Mokdad, A. H., Serdula, M. K., Dietz, W. H., Bowman, B. A., Marks, J. S. & Koplan, J. P. (1999) *J. Am. Med. Assoc.* **282,** 1519–1522.
2. Yip, J., Facchini, F. S. & Reaven, G. M. (1998) *J. Clin. Endocrinol. Metab.* **83,** 2773–2776.
3. Unger, R. H., Zhou, Y. T. & Orci, L. (1999) *Proc. Natl. Acad. Sci. USA* **96,** 2327–2332.
4. Alpert, M. A., Terry, B. E., Mulekar, M., Cohen, M., Massey, C. V., Fan, T. M., Panayiotou, H. & Mukerji, V. (1997) *Am. J. Cardiol.* **80,** 736–740.
5. Iida, M., Murakami, T., Ishida, K., Mizuno, A., Kuwajima, M. & Shima, K. (1996) *Biochem. Biophys. Res. Commun.* **224,** 597–604.
6. Phillips, M. S., Liu, A., Hammond, H. A., Dugan, V., Hey, P. J., Caskey, C. J. & Hess, J. F. (1996) *Nat. Genet.* **13,** 18–19.
7. Zhou, Y. T., Shimabukuro, M., Wang, M. Y., Lee, Y., Higa, M., Milburn, J., Newgard, C. B. & Unger, R. H. (1998) *Proc. Natl. Acad. Sci. USA* **95,** 8898–8903.
8. Zhou, Y. T., Wang, Z. W., Higa, M., Newgard, C. B. & Unger, R. H. (1999) *Proc. Natl. Acad. Sci. USA* **96,** 2391–2395.
9. Duke, R. C. & Sellins, C. B. (1989) in *Cellular Basis of Immune Modulation*, ed. Kaplan, J. C. (Liss, New York), pp. 311–314.
10. Shimabukura, M., Zhou, Y. T., Levi, M. & Unger, R. H. (1998) *Proc. Natl. Acad. Sci. USA* **95,** 2498–2502.
11. Perry, D. K. & Hannun, Y. A. (1999) *Trends Biochem. Sci.* **24,** 266–267.
12. Danno, H. Y., Jinko, Y., Budiyanto, S., Furikawa, Y. & Kimura, S. A. (1992) *J. Nutr. Sci. Vitaminol.* **38,** 517–521.
13. Tandler, B. (1990) *J. Electron Microsc. Tech.* **16,** 81–82.
14. Weibel, E. R. (1973) in *Principles and Techniques of Electron Microscopy Biological Application*, ed. Hayat, M. A. (Van Nostrand Reinhold, New York), pp. 237–296.
15. Lee, Y., Hirose, H., Ohneda, M., Johnson, J. W., McGarry, J. D. & Unger, R. H. (1994) *Proc. Natl. Acad. Sci. USA* **91,** 10878–10882.
16. Zhou, Y. T., Shimabukuro, M., Lee, Y., Koyama, K., Higa, M., Ferguson, T. & Unger, R. H. (1998) *Diabetes* **47,** 1904–1908.
17. Keller, H., Dreyer, C., Medin, J., Mahfoudi, A., Ozato, K. & Wahli, W. (1993) *Proc. Natl. Acad. Sci. USA* **90,** 2160–2164.
18. Shimabukuro, M., Zhou, Y. T., Levi, M. & Unger, R. H. (1998) *Proc. Natl. Acad. Sci. USA* **95,** 2498–2502.
19. Shimabukuro, M., Ohneda, M., Lee, Y. H. & Unger, R. H. (1997) *J. Clin. Invest.* **100,** 290–295.
20. Higa, M., Zhou, Y. T., Ravazzola, M., Baetens, D., Orci, L. & Unger, R. H. (1999) *Proc. Natl. Acad. Sci. USA* **96,** 11513–11518.
21. Bielawska, A. E., Shapiro, J. P., Jiang, L., Melkonyan, H. S., Piot, C., Wolfe, C. L., Tomei, L. D., Hannun, Y. A. & Umansky, S. R. (1997) *Am. J. Pathol.* **151,** 1257–1263.